Regular paper

Free-view Pixels of Elemental Image Rearrangement Technique (FPERT)

Jaehoon Lee[1], **Myungjin Cho[2]**, **Kotaro Inoue[2]**, **Masaharu Tashiro[1]**, and **Min-Chul Lee[1]***,
Member, KIICE

[1]Department of Computer Science and Electronics, Kyushu Institute of Technology, Fukuoka 820-8502, Japan
[2]Department of Electrical, Electronics, and Control Engineering, IITC, Hankyong University, Anseong 17579, Korea

Abstract

In this paper, we propose a new free-view three-dimensional (3D) computational reconstruction of integral imaging to improve the visual quality of reconstructed 3D images when low-resolution elemental images are used. In a conventional free-view reconstruction, the visual quality of the reconstructed 3D images is insufficient to provide 3D information to applications because of the shift and sum process. In addition, its processing speed is slow. To solve these problems, our proposed method uses a pixel rearrangement technique (PERT) with locally selective elemental images. In general, PERT can reconstruct 3D images with a high visual quality at a fast processing speed. However, PERT cannot provide a free-view reconstruction. Therefore, using our proposed method, free-view reconstructed 3D images with high visual qualities can be generated when low-resolution elemental images are used. To show the feasibility of our proposed method, we applied it to optical experiments.

Index Terms: Integral imaging, three-dimensional computational reconstruction, three-dimensional visualization

I. INTRODUCTION

Three-dimensional (3D) image sensing and visualization methods have recently been used in many different industries, e.g., unmanned autonomous vehicles, unmanned cameras, and medical imaging. Because 3D information of objects can be obtained, a more accurate pattern recognition can be achieved. However, in a conventional 3D reconstruction, only single fixed-view 3D images are provided. Therefore, a free-view reconstruction with various viewing angles may be required.

As a passive 3D imaging technique, integral imaging introduced by Lippman in 1908 [1] can provide full color, full parallax, and a continuous viewpoint without the need for special glasses or a coherent light source such as a laser.

Integral imaging can be used to record multiple view-point images from an object through a lenslet array. Such recorded images are called elemental images. Three-dimensional images can be generated using these elemental images during the display stage of integral imaging. However, there are certain problems inherent to integral imaging, namely, a low viewing resolution, a narrow viewing angle, and a shallow depth of focus. When an image sensor with a limited resolution and a large number of lenslets is used to capture such elemental images, the resulting 3D image has a very low viewing resolution. In addition, the reconstructed 3D images during the display stage of the integral imaging may not have accurate 3D information. Therefore, many researchers have reported the use of a computational volumetric reconstruction [2-7].

In general, integral imaging consists of two steps, namely,

pickup and reconstruction processes. During the pickup process, the image sensor records the light field coming from 3D objects through a lenslet array. This light field creates elemental images with different perspectives of 3D objects. In the classical reconstruction process, namely, volumetric computational reconstruction (VCR) [4], elemental images are back-projected onto the reconstruction plane through a virtual pinhole array to generate a 3D image. Here, the elemental images are rearranged by shifting the pixel values according to the reconstruction depth. In addition, the pixel density can be determined based on the number of overlaps. Finally, the average pixel values of the overlapped pixels on the reconstruction plane are calculated to obtain 3D images. This method can be implemented through a shift and sum of the elemental images and provides 3D images similar to those achieved using an optical reconstruction.

A VCR can provide free-view reconstructed 3D images [8-13]. However, it is slow and extremely complicated. In addition, when low-resolution elemental images are used, 3D images with a high visual quality cannot be obtained.

The pixels of elemental image rearrangement technique (PERT) [14, 15] can be used to reconstruct 3D images by rearranging the pixels of elemental images. Because it does not need to calculate the average pixel value from the overlapped pixels on the reconstruction plane, its processing speed is much faster than that of a VCR. In addition, it can reconstruct 3D images with a higher visual quality. However, it cannot obtain free-view reconstructed 3D images because it utilizes all elemental images (i.e., all viewing points). Therefore, to solve these problems, in this paper, we propose a new free-view computational reconstruction method based on PERT with locally selective elemental images (i.e., selective viewing points). We call our proposed method the free-view pixels of elemental image rearrangement technique (FPERT).

The remainder of this paper is organized as follows. In Section II, we introduce a VCR, PERT, and our proposed method. In Section III, we provide the experimental results proving that our method can obtain highly accurate free-view reconstructed 3D images even if low-resolution elemental images are applied. Finally, a summary and some concluding remarks are presented in Section IV.

II. FREE-VIEW PIXELS OF ELEMENTAL IMAGE REARRANGEMENT TECHNIQUE (FPERT)

Fig. 1 illustrates the basic concept of integral imaging. Integral imaging can be used to record a light field from a 3D object through a lenslet array during the pickup stage. Multiple view images (i.e., elemental images) for an object are recorded. The number of elemental images is determined based on the number of lenslets. A 3D image can then be displayed by back-projecting these elemental images through
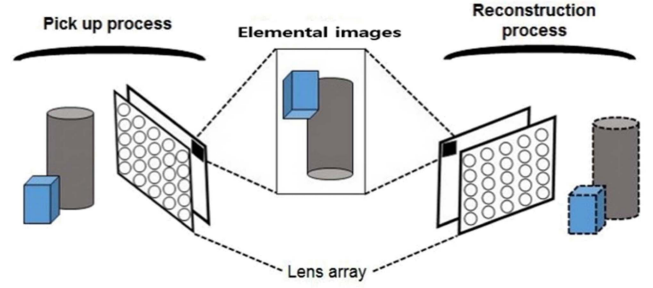

Fig. 1. Basic concept of integral imaging.

the homogenous lenslet array used during the pickup stage. However, to provide 3D information (or a 3D profile) of the object for various applications, a computational reconstruction may be required. In this section, we consider several computational reconstruction methods of integral imaging, such as a VCR and PERT.

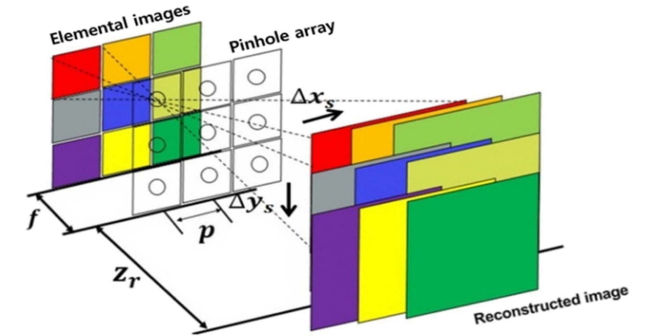### A. Volumetric Computational Reconstruction (VCR)

Fig. 2. Concept of VCR.

Fig. 2 shows the process of a VCR in which 3D images can be reconstructed using the back-projection of elemental images on the reconstruction plane through a virtual pinhole array based on the number of shifting pixels. Such numbers of shifting pixels, Δx_s and Δy_s, can be found based on the reconstruction depth, z_r.

$$\Delta x_s = \frac{E_x p_x f}{C_{sx} z_r}, \quad \Delta y_s = \frac{E_y p_y f}{C_{sy} z_r} \qquad (1)$$

where E_x and E_y are the numbers of pixels for each elemental image, p_x and p_y are the pitches between virtual pinholes, f is the distance between elemental images and the virtual pinhole array, and C_{sx} and C_{sy} are the image sensor sizes. Back-projected elemental images overlap each other on the reconstruction plane with pixilated Δx_s and Δy_s. Finally, the average values of the overlapped pixels on the reconstruction

plane (i.e., reconstructed 3D image), $I(x, y, z_r)$, can be calculated using

$$I(x,y,z_r) = \frac{1}{O(x,y,z_r)}\sum_{k=0}^{K-1}\sum_{l=0}^{L-1}I_{kl}(x+k\Delta x_s + l\Delta y_s) \quad (2)$$

where I_{kl} is the elemental image of the kth column and lth row, k, l is the index of elemental images, and $O(x, y, z_r)$ is the overlapping matrix.

However, the 3D images reconstructed using a VCR have only a single view (in general, a center view) because all pixels are concentrated on the center view of the elemental images. Therefore, to generate 3D images with various viewing points, free-view reconstruction methods are required.

In the free-view reconstruction of integral imaging, the reconstruction plane should typically be tilted [8]. To tilt the reconstruction plane, we need the locally nonuniform magnification ratio of each elemental image. This ratio is determined based on the ratio between the pickup and reconstruction planes. On the tilted reconstruction plane, different magnification ratios of each elemental image are used. Therefore, each elemental image can be transformed through an affine image transformation with different perspectives. Finally, we can effectively focus the free-view points of a 3D reconstruction image. However, this method requires a complicated image transformation algorithm, and the elemental images are distorted during the processing stage.

To simplify a free-view computational reconstruction, in this paper, locally selective elemental images (i.e., selective viewing points) are used. In addition, for a visual quality enhancement of the reconstructed 3D images, PERT is employed.

B. Pixels of Elemental Image Rearrangement Technique (PERT)

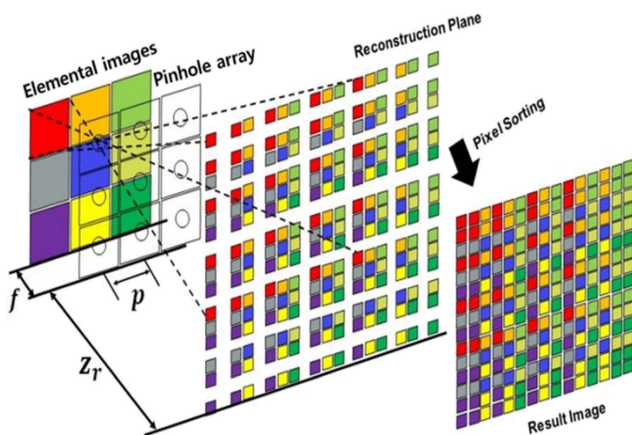Fig. 3 illustrates the process of PERT. It calculates the position of each pixel for the elemental images on the reconstruction plane through the virtual pinhole array, and then rearranges the pixels by sorting the positions of each pixel. Finally, reconstructed 3D images with an enhanced visual quality are obtained because it avoids the averaging effect (i.e., low-pass filtering) of a VCR. In addition, its processing speed is much faster than that of a VCR because it calculates and sorts the position of the pixels on the reconstruction plane.

To calculate the pixel position on the reconstruction plane, the magnification ratio M and the pixel size on the reconstruction plane x_r should be defined as follows:

$$M = \frac{Z_r}{f} \quad (3)$$

$$x_r = \frac{MC_{sx}}{KE_x}, \quad y_r = \frac{MC_{sy}}{LE_y} \quad (4)$$

$$R_{mk} = m \times \frac{x_r}{2} + k \times p_x, \quad \text{for} \quad \begin{matrix} m = 1,2,3,\dots,E_x \\ k = 0,2,3,\dots,K-1 \end{matrix}$$

$$R_{nl} = n \times \frac{y_r}{2} + l \times p_y, \quad \text{for} \quad \begin{matrix} n = 1,2,3,\dots,E_y \\ l = 0,2,3,\dots,L-1 \end{matrix} \quad (5)$$

We need to calculate the magnification ratio using the distance z_r and the camera focal length f. In addition, we define each projected pixel size, x_r, y_r, as shown in (4).

Then, the projection position of each pixel on the reconstruction plane, R_{mk} and R_{nl}, can be calculated using (5), where m, n is the pixel index for each elemental image. We defined new projection positions of all pixel arrangements as L_z. Finally, by sorting these projection positions of all pixels using a bubble sort algorithm [14], the reconstructed 3D images with a high visual quality can be obtained, as shown in Fig. 4.

With PERT, because only a positional calculation of all projected pixels and their position sorting are required, the processing speed is faster than that of a conventional VCR.
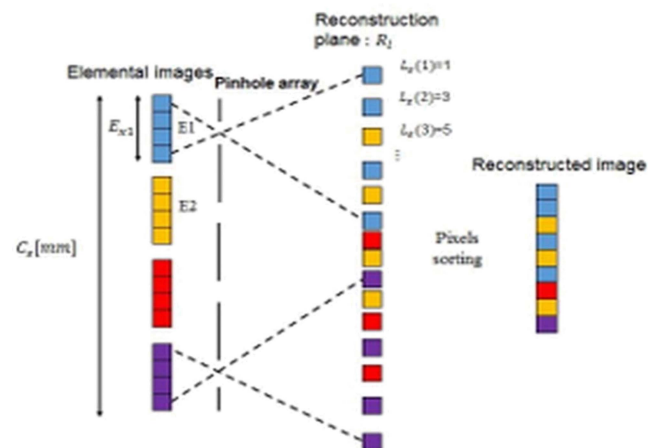

Fig. 3. Concept of PERT.

Fig. 4. Arrangement of x-axis pixels of PERT.

In addition, the visual quality is better than that of a conventional VCR because PERT does not calculate the average values among overlapped pixels. However, PERT has only a single view (particularly the center view). To generate reconstructed 3D images with a free view, in this study, we select elemental images corresponding to the viewing point. We then reconstruct 3D images with a free view using PERT.

C. Free-view Pixels of Elemental Image Rearrangement Technique (FPERT)

Fig. 5 illustrates the process used by FPERT. With the proposed method, we can choose pixels of the elemental image locally, and the pixels are projected onto the reconstruction plane through a virtual pinhole. After we choose the pixels of the elemental image, we calculate the position of each pixel and implement the same pixel rearrangement process used by PERT. In the pixel rearrangement, pixels have their own position numbers on the reconstruction plane. Using this pixel arrangement process, we can cluster the local elemental image pixels according to the viewing points. To rearrange these pixels, a new pixel rearrangement, U'_x and U'_y, should be defined using the following equations:

$$E_{xA} \leq U'_x \leq E_{xB} \ for\ A, B = 1, 2, 3,..., E_x \qquad (6)$$

$$E_{yC} \leq U'_y \leq E_{yD} \ for\ C, D = 1, 2, 3,..., E_y \qquad (7)$$

where A, B, C, and D are the group of local elemental image pixels. We can select the position of the elemental images by defining A, B, C, and D in (6) and (7). For these values, only a value of 1 to the value at the end of the elemental image index, E_x and E_y, can be selected. Group A should have a lower value than group B, and group C should have a lower value than group D. After selecting the group of pixels, we need to create a new pixel rearrangement, namely, U'_x and
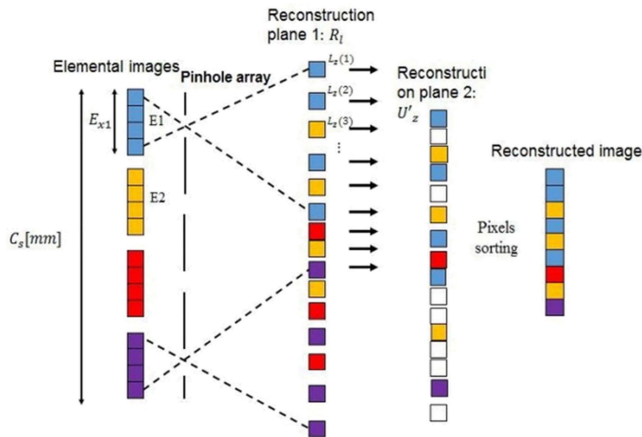
U'_y. Finally, a 3D reconstructed image can be generated using the same bubble sort algorithm as used by PERT.

For example, suppose we use elemental images in a 5×5 arrangement. For A, B, C, and D, we can choose values of 1 through 5 in the modified versions of (6) and (7). If numbers 1, 2, 1, and 2 are chosen for A, B, C, and D, FPERT generates an upper-left-side focused 3D reconstruction. In addition, if we want to focus on a certain part in detail, we can adjust the pixel arrangement of the elemental images locally. Using our proposed method, the free-view 3D reconstructed images with an enhanced visual quality can be generated without any complicated algorithms or image distortion.

III. EXPERIMENTAL RESULTS

To show the advantages of our proposed method, we use a 10 (H) $\times$ 10 (V) camera array with a focal length of 50 mm and pitch between cameras of 2 mm. We use a Nikon D3200 model camera in our experiment, which has a 23.2 mm $\times$ 15.4 mm sensor size. We used a toy car with the word "KYUTECH" printed on it. The distance between the toy car and the camera was set to 138 mm. Fig. 6 shows our experimental setup.

We captured high-resolution elemental images of 3,008 (H) $\times$ 2,000 (V) in size, but resized each elemental image to a size of 135 (H) $\times$ 90 (V) to show the ability of our proposed method to reconstruct 3D images with an enhanced visual quality even if low-resolution elemental images are applied. Fig. 7 shows the elemental images used in our
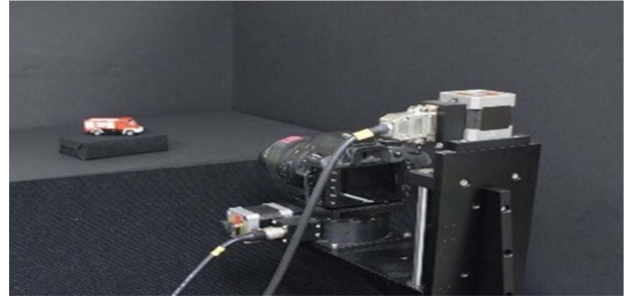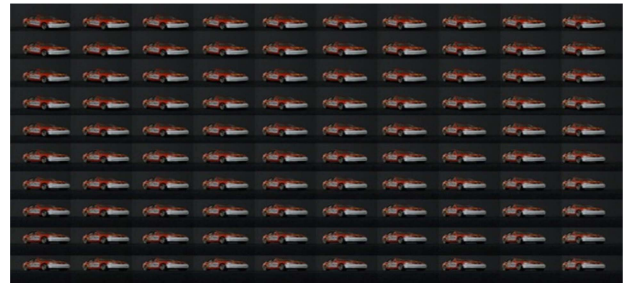

Fig. 6. Experiment setup.

Fig. 7. Elemental images.

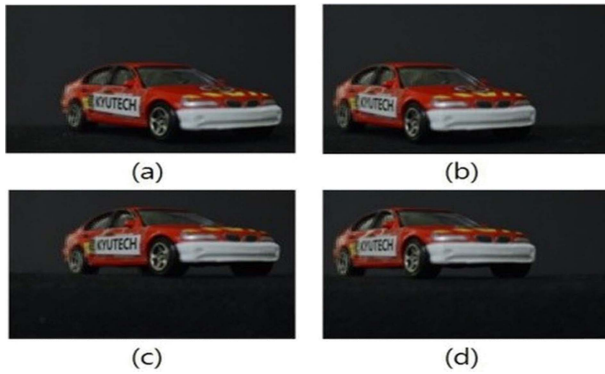**Fig. 5.** Arrangement of x-axis pixels of FPERT.

Fig. 8. FPERT results: (a) upper-left-side view, (b) upper-right-side view, (c) lower-side-view, and (d) lower-right-side view.
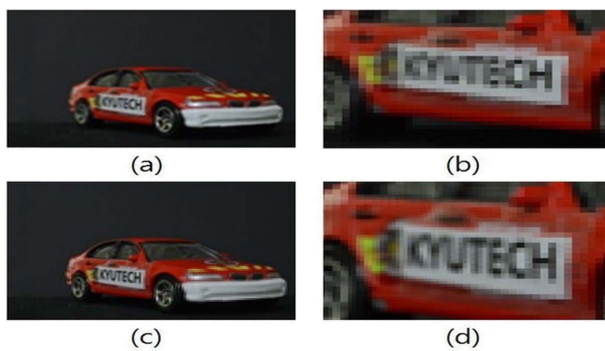

Fig. 9. VCR and FPERT results using 2 × 2 elemental images: (a) image reconstructed using a VCR, (b) enlarged VCR result, (c) reconstructed image using FPERT, and (d) enlarged FPERT result.

Fig. 10. Resulting images using VCR and FPERT: (a) resulting image (using 3 × 3 elemental images) from VCR, (b) enlarged resulting image using VCR, (c) resulting image from FPERT, and (d) enlarged resulting image using FPERT.

Fig. 11. Results of VCR and FPERT using 3 × 3 elemental images: (a) reference image with high resolution, (b) result using VCR, and (c) result using FPERT.

Fig. 12. Results of (a) PSNR, (b) SSIM, and (c) correlation peak.

experiment. Fig. 8 shows the results of FPERT for different viewing points of a 3D object. The reconstruction depth in our FPERT results is 147 mm.

Figs. 9 and 10 show the results of a VCR and our proposed method for comparison. We use the elemental images locally in a VCR to obtain free-view reconstructed images. For the VCR, we use 2 (H) × 2 (V) and 3 (H) × 3 (V) elemental images from the upper-left side of the elemental images. With our proposed method, we can extract the pixels locally from the elemental images. Thus, we do not need to crop the images.

To compare the visual quality of free-view reconstructed 3D images using both VCR and FPERT, we magnify the door part of the toy car, which has the word "KYUTECH" printed on it. It should be noted that FPERT can achieve a better visual quality of the reconstructed image. In Figs. 9 (b) and 10 (b), the word "KYUTECH" cannot be recognized in the image reconstructed using a VCR. In contrast, in Figs. 9 (d) and 10 (d), the word "KYUTECH" in the image reconstructed by FPERT can be better recognized than that reconstructed using a VCR.

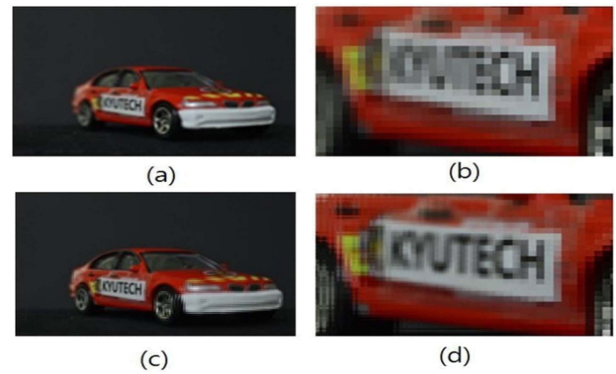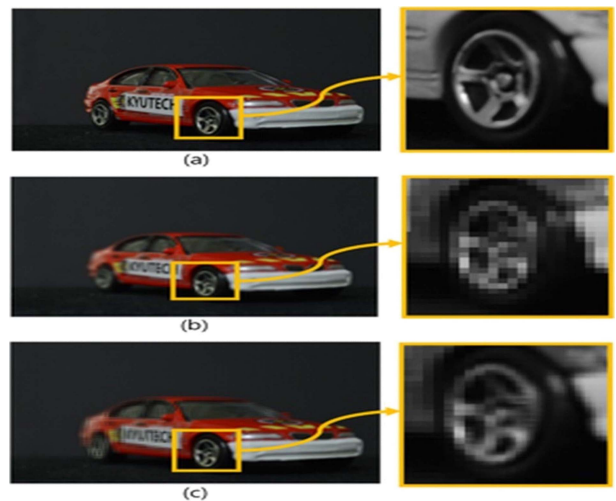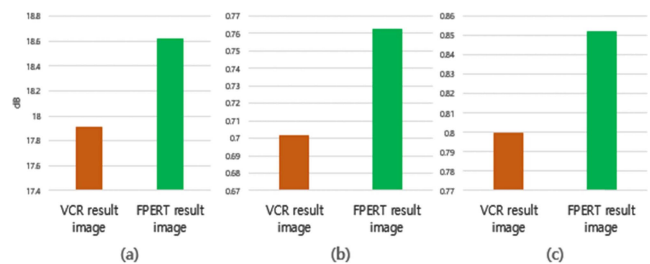In addition, Fig. 11 shows the tire of the toy car. We can recognize that our proposed method achieves a better image quality than that of a conventional method. In addition, we tested the image quality using the SSIM, PSNR, and a correlation. To test the results of the conventional method and our proposed method, we used a high-resolution 2D image of a toy car as a reference image. The reconstruction depth of all resulting images is 137 mm.

We used the same low-resolution elemental image as in Figs. 9 and 10. We can recognize the tire spokes well when using our proposed method. Fig. 12 shows that our proposed method can generate a higher quality image than that of a conventional method.

IV. DISCUSSION AND CONCLUSIONS

In this paper, we presented the proposed FPERT method and compared its results with those of a VCR. Although low-resolution elemental images are used, FPERT can generate free-view reconstructed 3D images with a better visual quality than those of a VCR. With a VCR, a complicated algorithm should be used, which can cause an image distortion during the reconstruction process. However, with FPERT, free-view 3D reconstructed images can be expressed using the local pixel rearrangement without the need for a complicated process. Therefore, our proposed method can enhance the processing speed and visual quality of a reconstructed 3D image. However, a problem of our proposed method is the distance between the camera and object. Because only a portion of the pixels of the element image is used, we cannot see the entire object when it is too close to the camera. We plan to investigate a solution to this problem in a future study.

ACKNOWLEDGEMENTS

REFERENCES

[1] G. Lippmann, "Epreuves reversibles. Photographies integrals," *Comptes-Rendus Academie des Sciences*, vol. 146, pp. 446-451, 1908.

[2] A. Stern and B. Javidi, "Three-dimensional image sensing, visualization, and processing using integral imaging," *Proceedings of the IEEE*, vol. 94, no. 3, pp. 591-607, 2006. DOI: 10.1109/JPROC.2006.870696.

[3] H. Arimoto and B. Javidi, "Integral three-dimensional imaging with computed reconstruction," *Optics Letters*, vol. 26, no. 3, pp. 157-159, 2001. DOI: 10.1364/OL.26.000157.

[4] S. H. Hong, J. S. Jang, and B. Javidi, "Three-dimensional volumetric object reconstruction using computational integral imaging," *Optics Express*, vol. 12, no. 3, pp. 483-491, 2004. DOI: 10.1364/OPEX.12.000483.

[5] J. S. Jang and B. Javidi, "Improved viewing resolution of three-dimensional integral imaging bu use of nonstationary micro-optics," *Optic Letters*, vol. 27, no. 2, pp. 324-326, 2002. DOI: 10.1364/OL.27.000324.

[6] D. H. Shin and H. Yoo, "Image quality enhancement in 3D computational integral imaging by use of interpolation methods," *Optics Express*, vol. 15, no. 19, pp. 12039-12049, 2007. DOI: 10.1364/OE.15.012039.

[7] J. S. Jang and B. Javidi, "Three-dimensional synthetic aperture integral imaging," *Optic Letters*, vol. 27, no. 13, pp. 1144-1146, 2002. DOI: 10.1364/OL.27.001144.

[8] M. J. Cho and B. Javidi, "Free view reconstruction of three-dimensional integral imaging using tilted reconstruction planes with locally nonuniform magnification," *Journal of Display Technology*, vol. 5, no. 9, pp. 345-349, 2009 DOI: 10.1109/JDT.2009.2028035.

[9] M. C. Lee, J. S. Han, and M. J. Cho, "3D visualization technique for occluded objects in integral imaging using modified smart pixel mapping," *Journal of Information and Communication Convergence Engineering*, vol. 15, no. 4, pp. 256-261, 2017. DOI: 10.6109/jicce.2017.15.4.256.

[10] Y. S. Hwang, S. H. Hong, and B. Javidi, "Free view 3D visualization of occluded objects by using computational synthetic aperture integral imaging," *Journal of Display Technology*, vol. 3, no. 1, pp. 64-70, 2007. DOI: 10.1109/JDT.2006.890702 .

[11] D. H. Shin, B. G. Lee, and E. S. Kim, "Modified smart pixel mapping method for displaying orthoscopic 3D images in integral imaging," *Optics and Lasers in Engineering*, vol. 50, no. 6, pp. 862-868, 2012. DOI: 10.1016/j.optlaseng.2009.06.004.

[12] B. H. Lee, S. Y. Jung, and J. H. Park, "Viewing-angle-enhanced integral imaging by lens switching," *Optical Letters*, vol. 27, no. 10, pp. 818-120, 2002. DOI: 10.1364/OL.27.000818.

[13] M. C. Lee, K. Inoue, and M. J. Cho, "Three-dimensional automatic target recognition system based on optical integral imaging," *Journal of Information and Communication Convergence Engineering*, vol. 14, no. 1, pp. 51-56, 2016 DOI: 10.6109/jicce.2016.14.1.051.

[14] M. J. Cho and B. Javidi, "Computational reconstruction of three-dimensional integral imaging by rearrangement of elemental image pixels," *Journal of Display Technology*, vol. 5, no. 2, pp. 61-65, 2009. DOI: 10.1109/JDT.2008.2004857.

[15] K. Inoue, M. C. Lee, B. Javidi, and M. J. Cho, "Improved 3D integral imaging reconstruction with elemental image pixel rearrangement," *Journal of Optics*, vol. 20, no. 2, pp. 8, 2018. DOI: 10.1088/2040-8986/aaa391.
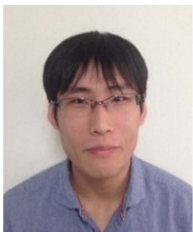
Jaehoon Lee

received the B.S. degrees from Hankyong National University, Korea, in 2018. He is a master's student at Kyushu Institute of Technology in Japan. His research interests are areas of Integral imaging, three dimensional computational reconstruction, Digital holographic microscopy and three dimensional visualization.

Myungjin Cho

received the B.S. and M.S. degrees in Telecommunication Engineering from Pukyong National University, Pusan, Korea, in 2003 and 2005, and the M.S. and Ph.D. degrees in electrical and computer engineering from the University of Connecticut, Storrs, CT, USA, in 2010 and 2011, respectively. Currently, he is an associate professor at Hankyong National University in Korea. He worked as a researcher at Samsung Electronics in Korea, from 2005 to 2007. His research interests include 3D display, 3D signal processing, 3D biomedical imaging, 3D photon counting imaging, 3D information security, 3D object tracking, 3D underwater imaging, and 3D visualization of objects under inclement weather conditions.

Kotaro Inoue

received the B.S. and M.S. degrees in computer science and electronics from Kyushu Institute of Technology, Fukuoka, Japan, in 2015 and 2017, respectively. He is currently a doctoral student at Hankyong National University in Korea. His research interests include visual feedback control, 3D display, 3D reconstruction, and 3D integral imaging.

Masaharu Tashiro

received the B.S. degrees from Kyushu Institute of Technology, Fukuoka, Japan, in 2018. He is a master's student at Kyushu Institute of Technology in Japan. His research interests are areas of biological imaging, 3D display, and 3D integral imaging.

Min-Chul Lee

received the B.S. degrees in Telecommunication Engineering from Pukyong National University, Busan, Korea, in 1996, and the M.S. and Ph.D. degrees from Kyushu Institute of Technology, Fukuoka, Japan, in 2000 and 2003, respectively. He is an assistant professor at Kyushu Institute of Technology in Japan. His research interests include medical imaging, blood flow analysis, 3D display, 3D integral imaging, and 3D biomedical imaging.